Applied Clay Science xxx (2015) xxx–xxx

Contents lists available at ScienceDirect

Applied Clay Science

journal homepage: www.elsevier.com/locate/clay

Spheroidal halloysites from Patagonia, Argentina: Some aspects of their formation and applications

CraveroF. [a,b,*], FernándezL. [c], MarfilS. [d,e], SánchezM. [c], MaizaP. [e], MartínezA. [f]

[a] Centro de Tecnología de materiales y cerámica, CETMIC, CONICET-CIC, Centenario Av. and 506, Gonnet, La Plata, Argentina
[b] CONICET, Rivadavia Av., 1917, Argentina
[c] Chemistry Department, College of Engineering, Universidad Nacional del Comahue, Buenos Aires 1400, Neuquén, Argentina
[d] CIC of the Province of Buenos Aires, 526 St. between 10 and 11, Argentina
[e] Geology Department, Universidad Nacional del Sur, San Juan 670, Bahía Blanca, Argentina
[f] Biotec Argentina S.R.L., Parque Industrial Cinco Saltos, Río Negro, Argentina

ARTICLE INFO

Article history:
Received 19 June 2015
Received in revised form 11 January 2016
Accepted 13 January 2016
Available online xxxx

Keywords:
Spheroidal halloysite
Weathering
Chemical modification

ABSTRACT

Halloysite deposits in Argentina have been identified in the province of Río Negro (Patagonia). The mineralized area occurs as altered zones in Eocene volcanic–pyroclastic rocks, dacitic to rhyolitic in composition. A comprehensive study of these deposits was carried out by means of mineralogical, geochemical and isotopic analyses. Intense weathering has transformed the whole rock to a white mass composed of 75% –90% halloysite + kaolinite, with cristobalite, tridymite, and quartz, as the main non-clay minerals. Ferruginous beidellite and titanium minerals are also present in minor amounts.

The halloysite–kaolinite ratio ranges from 75 to 25 to 100–0. Due to the alteration of very dense rocks, halloysite morphology is predominantly spheroidal. Tubular halloysite is the main constituent in more porous rocks, but the latter are scarce in the area.

Because of the predominance of the spheroidal type, the use of halloysite as HNT (halloysite nanotube) is not feasible. Nonetheless, this mineral can be modified by different organic molecules, and used to remove pollutants such as emulsified hydrocarbons and heavy metals. A special product made with this halloysite is used as sunscreen when sprayed on fruits in areas of intense solar radiation. The whiteness of this mineral is not very high due to the amount of titanium oxide present in its composition (about 1%). Nevertheless, titanium oxide is present as individual particles, so it could be removed by a mechanical process.

New applications for spheroidal halloysite are currently being investigated. Moreover, depending on the price and demand, the tubular halloysite of low grade deposits could be exploited.

1. Introduction

Halloysite is defined by the presence or evidence of past occurrence of interlayer water in a mineral with a kaolin-type structure (Churchman and Carr, 1975). Halloysite and kaolinite have identical chemical composition, being composed of aluminosilicate layers comprising $Al_2Si_2O_5(OH)_4$, except that halloysite may have as many as two molecules of H_2O, as interlayer water, for each $Al_2Si_2O_5(OH)_4$ (Churchman et al., 2010). The content of additional water in the interlayers has a decisive influence upon its crystal morphology, which is generally curled rather than platy as in kaolinite. Common forms are elongated tubes and spheroids.

The tubular morphology makes this mineral attractive as specialty clay, in fact a trademark product called HNT has been released. Unfortunately, the large deposits from which pure tubular halloysite can be economically extracted are comparatively rare (Keeling, 2015). Only two high grade deposits are known: one in Northland, New Zealand, from weathered rhyolite, and the other in the Tintic district of Utah, United States of America, from hydrothermal clay masses replacing dolomite. Smaller or lower grade deposits occur in Japan, Korea, China, Thailand, Indonesia, Australia, South America, and Europe.

In Argentina, small and low grade deposits are located in the area of Mamil Choique and Buitrera, Patagonia, Argentina (Cravero et al., 2009, 2012). In Mamil Choique, the deposits are not small but spheroids predominate over tubes, whereas in Buitrera, the deposit is small and tubes predominate over spheroids. Mamil Choique and Buitrera are 50 km apart in a W–E direction in a similar geological environment. In between, there are several localities where the rocks are also altered to halloysite. The extension of the alteration, the high halloysite/rock ratio, not common in this type of deposit, and the formation of halloysite rather than kaolinite in different rocks at the same time and with different morphologies make these areas of interest to contribute to the understanding of the formation conditions of halloysite (Cravero et al., 2012).

* Corresponding author at: Centro de Tecnología de materiales y cerámica, CETMIC, CONICET-CIC, Centenario Av. and 506, Gonnet, La Plata. Argentina.
E-mail address: fcravero@cetmic.unlp.edu.ar (F. Cravero).

http://dx.doi.org/10.1016/j.clay.2016.01.011
0169-1317/

Taking into consideration that spheroids are the predominant morphology, some attempts were made in order to determine possible applications of these halloysites (Fernández et al., 2009a, 2009b, 2013, 2015).

This work contributes to clarifying the supergenic or hypogenic origin of halloysite, and is intended to present possible applications of the actually mined area. To carry on this study, XRD, DTA-TG, chemical and isotopic analyses, petrography, surface chemical modifications, and technological measurements were all used.

2. Materials and methods

Past detailed studies on different parts of Mamil Choique and Buitrera deposits demonstrated that the mineralogy in the Mamil Choique deposits comprises halloysite, kaolinite, with impurities such as tridymite, cristobalite, quartz, iron-rich beidellites, and iron oxides. In Buitrera, halloysite, along with cristobalite and tridymite, is the main component (Cravero et al., 2009, 2012, 2014a).

To determine the mineralogical and chemical variations of the altered areas, samples were collected along all the fronts of exploitation in the mined area (Pama), in all the other deposits nearby Pama (Rosas, San Martín, Santiago, Urquiza) as well as in the different small deposits (Meliqueo, Alfa) located in between Mamil Choique and Buitrera.

To evaluate the industrial application of the biggest deposit (Pama), a composite whole rock sample (Comp Sample), obtained by blending samples from different exploitation fronts, was homogenized and ground as the material that is currently commercialized. This material was subdivided into subsamples to be characterized by different methods. The mineralogy as well as chemical composition were determined on the obtained samples.

The mineralogy was ascertained through a combination of X-Ray diffraction (XRD), Scanning and Trasmition Electron Microscopes (SEM and TEM) analyses. XRD was performed on a whole sample, and the mineral content was evaluated with the computer program SIROQUANT. Oriented samples were analyzed before and after formamide intercalation, and the halloysite/kaolinite ratio was determined (Churchman et al., 1984). Halloysite morphology was evaluated by SEM and TEM.

Chemical analyses for major and minor elements, as well as oxygen and hydrogen isotopic composition, were performed by Inductevely Coupled Plasma (ICP) at Activation Laboratories Ltd. (Actlabs, Canada). The latter is shown as deviation relative to SMOW ‰, and the reproducibility of the results is greater than 0.5 ‰–10 ‰ or H. Grain size distribution was measured with a Micromeritics sedigraph, Sedi-Graph 5000, and ceramic evaluation was made at Instituto Nacional del Tecnología Industrial (National Institute for Industrial Technology, INTI) labs in Buenos Aires city.

The Comp Sample was modified with different organic compounds to obtain a product able to extract metallic elements from suspensions. The chemical composition was determined by X-Ray Fluorescence (XRF) with a dispersive energy spectrometer, Shimadzu 800HS, using the method of fundamental parameters, and Infra Red Spectrometry (IR) was performed with a Lumex FT08. Differential Thermal Analysis and Thermogravimetric (DTA and -TG) analyses were performed in a Rigaku Evo II Series TG8120 device at a heating rate of 10 °C/min from room temperature up to 1000 °C under O_2 atmosphere.

3. Results and discussion

3.1. Alteration

3.1.1. Characterization

Large and small “pockets” of rocks altered to halloysite are found along a 50 km area in a W–E direction, but no structural control has been detected (Fig. 1). In Mamil Choique, these pockets (Fig. 2) are actually the different deposits and are normally flanked by fresh rocks. The altered zones are mainly composed of halloysite or kaolinite, with variable amounts of tridymite-cristobalite, quartz, feldspars, and traces of smectite (Fig. 3, Table 1).

Halloysite is found when the source is a pyroclastic rock, as in almost all the deposits in Mamil Choique, Meliqueo, Alfa and Buitrera. Cravero et al. (2012) indicated that probably waters circulating towards small basins filled with these rocks (thus giving the current pocket shape of the deposits) came into contact with them for long periods of time, and halloysite formed after the dissolution of glass. In Urquiza, where kaolinite predominates, the parent rock is acid plutonic (granite, granodiorite). Here, kaolinite is found as plates stacked as worms as in altered feldspar.

Although halloysite is the main alteration product in all the deposits, there is a variation in morphology among the different localities. Spheroidal halloysite predominates in the Mamil Choique area (Fig. 4a), whereas in Meliqueo, Alfa and Buitrera tubular halloysite is found (Fig. 4b, c and d, respectively). Why spheroidal halloysite forms is a matter of discussion, and different modes of origin have been proposed. Nagasawa (1978); Tomura et al. (1985); Quantin et al. (1988), Bailey (1989), Adamo et al. (2001); Singer et al. (2004); Churchman and Lowe (2012) considered that spheroidal halloysite comes from a fast dissolution of volcanic glass that results in a supersaturated solution which favors the formation of this particular shape. Also, it can be texturally constrained as in pumice cavities (Adamo et al., 2001). The origin of spheroidal halloysite from the transformation of allophane has been proposed by different authors. Askenasy et al. (1973) associated spheroidal halloysite with allophane interlayers that can be preserved in soils because the crystalline exterior layers protect it. Nagasawa and Miyazaki (1976) -, found that spheroidal halloysites, sometimes associated with short tubes, form by replacement of either volcanic glass or allophane. Sudo and Yotsumoto (1977) observed a variation in particle shape with burial depth: allophane aggregates coagulate to form spheroidal halloysite, downward transformed into tubular crystals. Tazaki (1982) indicated a transformation of an allophane into spheroidal particles. Spheroidal halloysite was also related to Fe content. Nagasawa and Moro (1987); Tazaki (1982); Churchman and Theng (1984); Singer et al. (2004) noticed that spheroidal forms have higher Fe content than tubular ones. Such trend is not found in other cases such as those studied by Soma et al. (1992), Adamo et al. (2001). Even a biogenic origin was proposed by Tazaki and Asada (2003), who observed that a spheroidal halloysite is formed by bacterial activities in freshwater and natural sediment systems at room temperature. The transformation of spheroidal halloysite to tubular halloysite in weathering profiles was well described by Sudo and Yotsumoto (1977) and Papoulis et al. (2004). The latter paper also concluded that there is an increase in the substitution of Al by Fe as the spheroidal halloysite transforms into tubular and platy forms. Cravero et al. (2012) concluded that in Mamil Choique and Buitrera deposits, halloysite is formed from the dissolution of volcanic glass and that the particle morphology depends on the original texture of the rock; spheroidal halloysite is related to rocks with low porosity, and tubular particles are related to rocks with open spaces similar to what was found by Adamo et al. (2001). Halloysite coming from different deposits has low iron content, and there are no differences associated with different morphologies. Higher iron values are related to the presence of smectite (Table 1). Smectite, a ferruginous beidellite, is formed with the iron released from the process that formed the halloysite (Cravero et al., 2014a). Further investigations might be carried out in order to establish the relationship of spheroidal and tubular halloysites when they are coexisting in some parts of the Santiago deposit (Table 1) and to determine if, although the halloysite formed in the early Paleocene (this paper), there is still evidence of allophane.

Also, the presence of kaolinite is constrained by the source rock, since it is formed from the alteration of feldspars of plutonic rocks (Urquiza).

Please cite this article as: Cravero, F., et al., Spheroidal halloysites from Patagonia, Argentina: Some aspects of their formation and applications, Appl. Clay Sci. (2015), http://dx.doi.org/10.1016/j.clay.2016.01.011

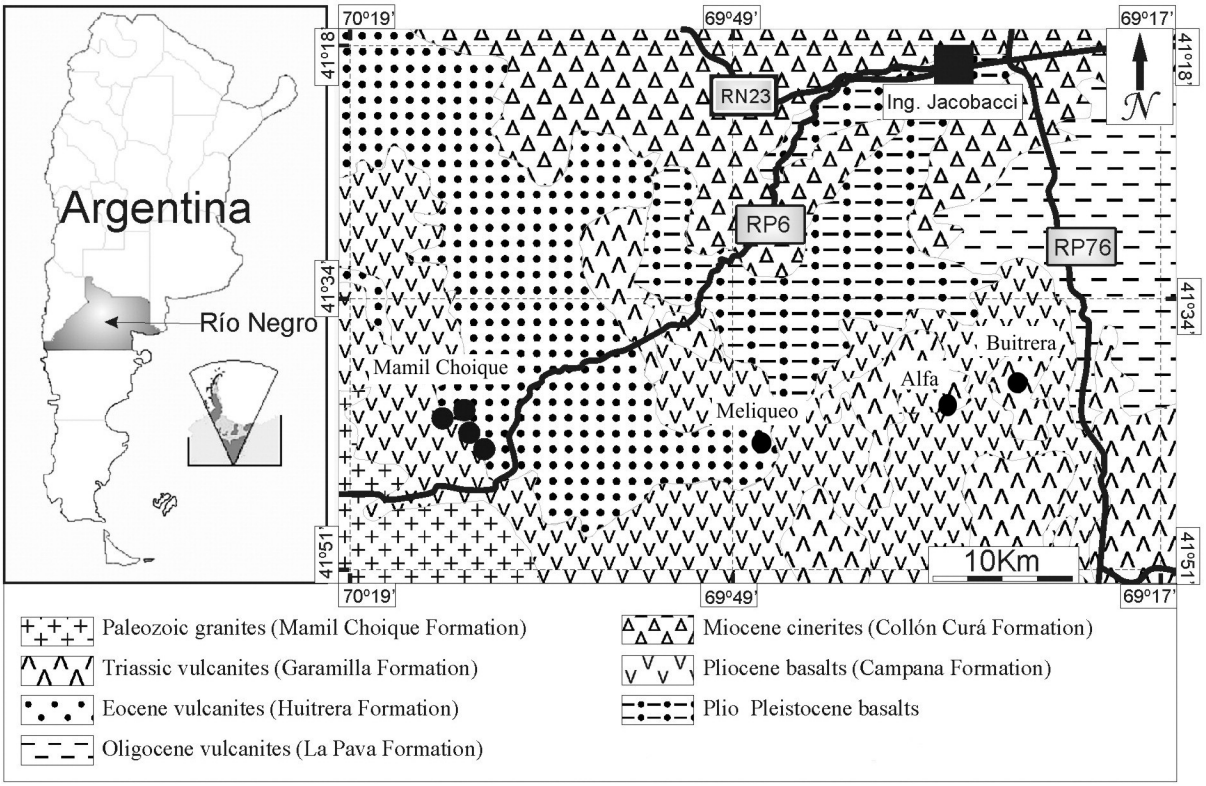

Fig. 1. Geological and geographical setting of the study area (Cravero et al., 2014a).

3.1.2. Supergenic or hypogenic origin

Dill et al. (1997) used the ratios SO_3 vs. P_2O_3, Zr vs. TiO_2, $TiO_2 + Fe_2O_3$ vs. Cr + Nb, and Ba + Sr vs. Ce + Y + La to separate kaolin deposits of different origins in Peru. They found that S, Ba and Sr are enriched during hydrothermal alteration, whereas Cr, Nb, Ti and lanthanide elements are concentrated mainly during weathering.

Condie et al. (1995) reported that Rb, Zr, Sc, Cr, Co, Hf, Nb, Ta, Y, Th, U, and REE are concentrated in the upper parts of a weathering profile developed on a granodiorite. Galán et al. (2007) indicated that variable amounts of Si, Na, Ca, K, Rb, Cs, Ba, U, and P have been lost from the weathering profile of granitic rocks in Spain, whereas Al, Fe, Ti, Zr, Th, Hf, and REE concentrate in the residual kaolin.

It is clear that some elements are mobile no matter the environment, such as Si, Na, Ca, K Rb and Cs, Ba and Sr. REE appear to concentrate during weathering and remain immobile under hypogene conditions.

Zr vs. TiO_2, $TiO_2 + Fe_2O_3$ vs. Cr + Nb and Ce + Y + La vs. Ba + Sr plots for the mines studied are shown in Fig. 5. Source rock compositions are also plotted to evaluate the enrichment or depletion of the elements. There is a clear depletion of Ba + Sr in all the deposits, as compared to the source rock.

TiO_2 and Zr show a tendency to concentrate during the alteration, Zr and TiO_2 contents show a positive linear correlation with the lower values of both elements in samples from the Buitrera mine due to their low degree of alteration. Zr concentration ranges between 186

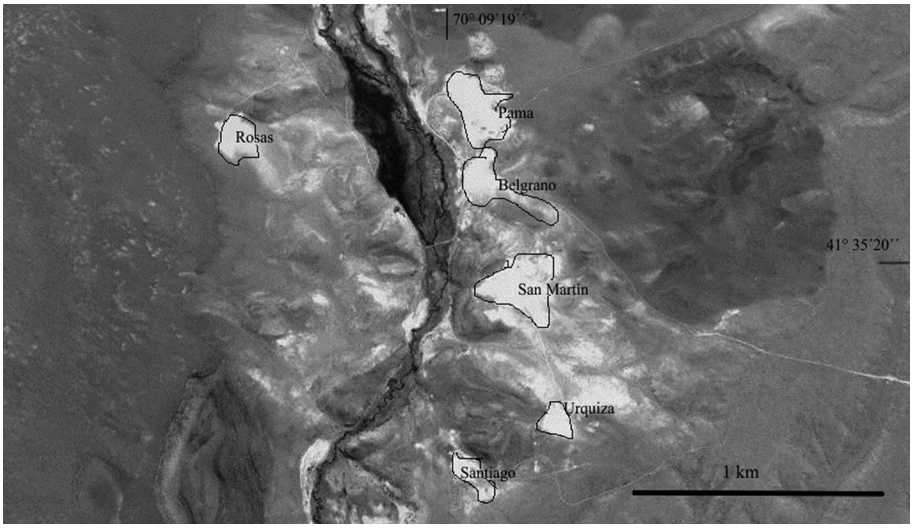

Fig. 2. Different quarries in Mamil Choique area.

Please cite this article as: Cravero, F., et al., Spheroidal halloysites from Patagonia, Argentina: Some aspects of their formation and applications, Appl. Clay Sci. (2015), http://dx.doi.org/10.1016/j.clay.2016.01.011

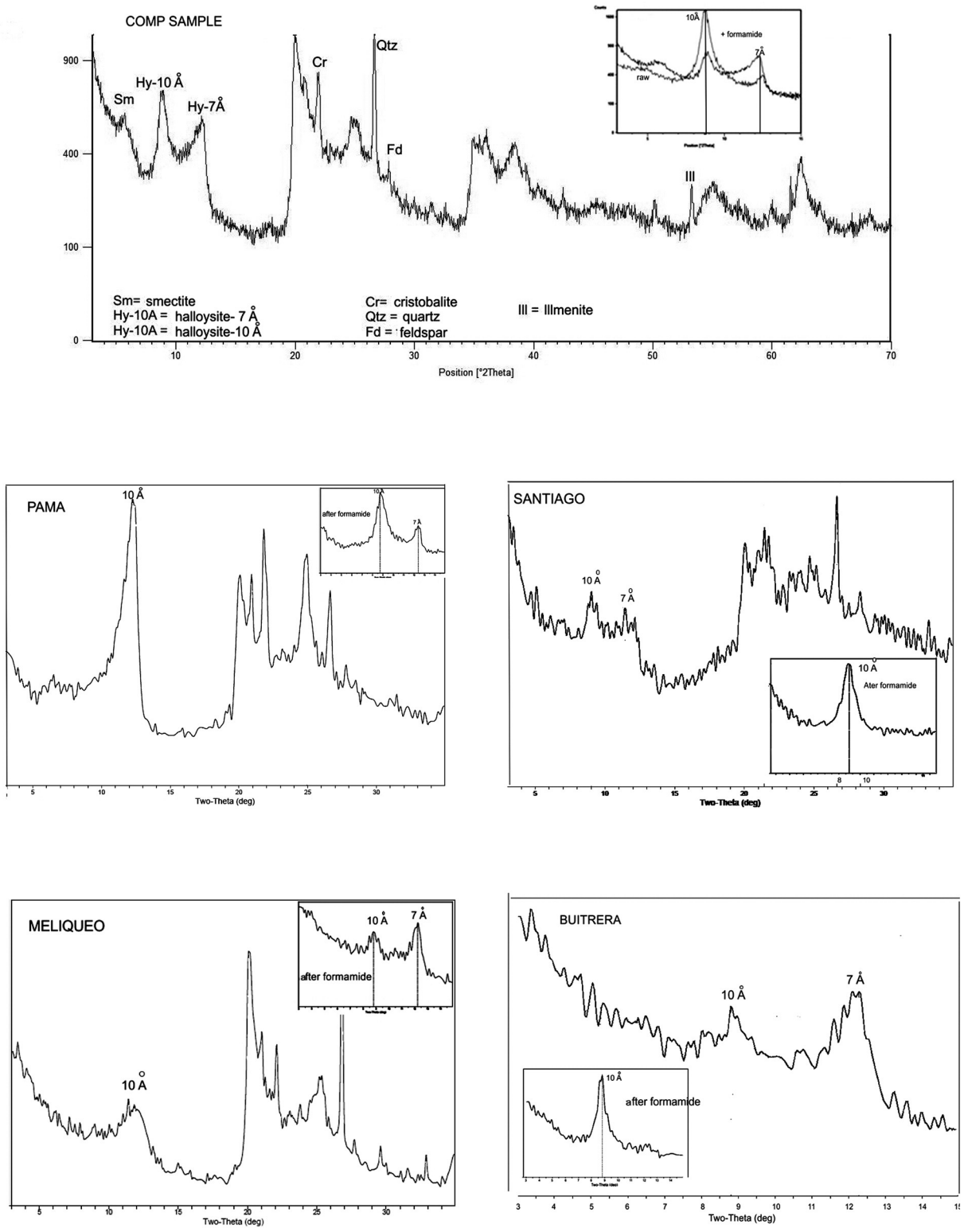

Fig. 3. XRD of the alterated zones showing the samples before and after formamide intercalation.

and 1080 ppm. $TiO_2 + Fe_2O_3$ contents are higher than 1% by weight, in accordance with the meteoric origin, and Cr + Nb range from 11 to 205 ppm with significant differences between samples from Mamil Choique and Buitrera.

Lantanide behavior is not clear. It is difficult to evaluate its role in Buitrera since the rocks are poorly altered. Depletion in LREE and enrichment in HREE have been observed in some samples from Alfa and Meliqueo. The strong Eu anomaly in several samples, mainly in the Buitrera area, implies that these rocks are from a felsic melt where feldspar was removed, or from the partial melting of a rock where the feldspar was retained at the source (Rollinson, 1992). Samples that do not show this strong anomaly come from the alteration of rocks composed of crystaloclasts of feldspar and plagioclase. When these rocks undergo an alteration process, Eu is not mobile, so the altered rocks must show

Please cite this article as: Cravero, F., et al., Spheroidal halloysites from Patagonia, Argentina: Some aspects of their formation and applications, Appl. Clay Sci. (2015), http://dx.doi.org/10.1016/j.clay.2016.01.011

Table 1
Chemical analysis of major and minor elements of the studied samples (in %); halloysite/kaolinite % in the whole sample and mineral associations.

Mine/Sample	SiO_2	Al_2O_3	Fe_2O_3	MnO		CaO	MgO	K_2O	TiO_2	P_2O_5	LOI	% Hall	Shape	Min
Pama1	43.57	29.41	1.36	0.009	0.24	0.30	0.12	0.24	0.93	0.06	23.44	75,12	Spheroidal	H-K /Qt Cr, Sm
Pama2	42.61	28.36	1.21	0.007	0.12	0.19	0.08	0.08	1.67	0.04	23.88	72,44	Spheroidal	H-K /Qt Cr, Sm
Pama3	40.85	28.65	0.67	0.006	0.12	0.20	0.17	0.24	1.49	0.02	27.23	73,18	Spheroidal	H-K /Qt Cr
Pama4	43.61	34.24	0.79	0.009	0.11	0.20	0.12	0.08	1.41	0.05	17.95	87,46	Spheroidal	H-K /Qt Cr
Pama5	48.68	32.08	0.50	0.005	0.22	0.26	0.25	0.18	1.19	0.03	15.29	81,94	Spheroidal	H-K /Qt Cr
Pama6	47.77	31.70	1.72	0.007	0.24	0.44	0.20	0.20	1.31	0.05	16.45	80,97	Spheroidal	H-K /Qt Cr, Sm
Santiago1	47.72	27.25	0.81	0.021	0.25	0.25	0.18	0.16	1.97	<0.01	19.94	69,6	Spheroidal	H-K /Qt Cr
Santiago2	40.02	30.13	0.67	0.006	0.17	0.24	0.17	0.06	1.17	0.03	26.87	76,96	Sph/tubular	H-K /Qt Cr
Santiago3	40.42	28.80	0.80	0.011	0.21	0.26	0.24	0.08	1.423	0.03	26.34	73,56	Tubular	H-K /Qt Cr
Santiago4	41.83	28.97	1.10	0.007	0.27	0.34	0.24	0.11	1.76	0.03	24.07	74	Spheroidal	H-K /Qt Cr
Santiago5	39.50	28.94	0.57	0.007	0.21	0.24	0.30	0.17	1.32	0.02	28.61	73,92	Tubular	H-K /Qt Cr
Santiago6	41.62	29.93	0.81	0.01	0.25	0.33	0.17	0.08	1.57	<0.01	25.47	76,45	Sph/tubular	H-K /Qt Cr
Santiago7	38.56	29.03	0.69	0.008	0.18	0.26	0.24	0.09	1.44	0.04	28.39	74,15	Spheroidal	H-K /Qt Cr
Santiago8	38.63	28.87	0.74	0.006	0.19	0.25	0.23	0.08	1.78	0.06	27.95	73,74	Tubular	H-K /Qt Cr
Urquiza1	47.45	29.12	3.78	0.013	0.45	0.46	0.22	0.18	0.20	0.07	17.2			H-K/Cr, Fd, Sm
Urquiza2	49.55	30.56	4.27	0.003	0.32	0.38	0.19	0.20	0.17	0.04	14.78			H-K/Cr, Fd, Sm
Rosas	45.98	27.37	0.90	0.006	1.43	0.59	0.17	0.10	0.43	0.05	21.76			H-K-Qtz-Cr-Fd-
San Martín	44.04	32.47	0.74	0.007	0.15	0.19	0.27	0.08	1.46	0.01	20.22	82,94	Spheroidal	H-K-Cr-Qtz-
Meliqueo1	44.65	31.54	0.65	0.012	0.18	0.33	0.40	0.35	1.43	0.07	20.45	80,56	Tubular	H-K-Qz-Fd-Cr-
Meliqueo2	48.56	26.93	1.70	0.01	0.64	0.85	0.38	0.82	1.25	0.06	18.18		Tubular	Qz-Fd-Cr-carb-H-K
Alfa1	43.56	29.63	4.60	0.087	0.85	0.46	0.28	0.20	0.96	0.06	19.91		Tubular	H-K/Cr, Fd, Sm
Alfa2	56.55	23.64	1.63	0.075	0.34	0.51	3.02	4.63	1.18	0.06	9.23		Tubular	H-K/Cr, Fd, Sm
Alfa3	49.00	27.23	2.95	0.021	0.38	0.32	1.29	2.22	1.247	0.07	15.55		Tubular	H-K/Cr, Fd, Sm
Alfa4	48.71	29.60	1.27	0.03	0.25	0.32	1.45	2.29	0.61	0.02	15.29		Tubular	H-K/Cr, Fd, Sm
Buitrera1	75.31	13.89	0.67	0.008	0.12	0.13	3.07	3.25	0.14	<0.01	3.95		Tubular	Cr-Fd minor Qtz
Buitrera2	76.87	13.36	0.62	0.009	0.08	0.10	3.20	3.49	0.14	0.02	2.52		Tubular	Tr-Cr-Fd- Qtz
Buitrera3	74.94	14.48	0.57	0.009	0.10	0.19	2.97	3.31	0.14	0.01	3.65		Tubular	Cr-Fd- Qtz
Mine/Sample	SiO_2	Al_2O_3	Fe_2O_3	MnO		CaO	MgO	K_2O	TiO_2	P_2O_5	LOI		Tubular	Min
Buitrera4	73.7	17.24	0.68	0.014	0.12	0.12	0.74	0.5	0.19	0.01	7.57		Tubular	Cr- Fd - H-K
Buitrera5	68.48	18.39	1.20	0.037	0.14	0.13	0.6	0.37	0.18	<0.01	8.69		Tubular	Cr-Fd- Qtz-H-K
Buitrera6	71.81	17.00	1.12	0.044	0.15	0.16	0.73	0.48	0.176	<0.01	8.01		Tubular	Cr-Fd- Qtz-H-K
Buitrera7	59.89	15.12	1.40	0.005	0.49	7.23	1.30	0.60	0.07	0.03	14.74		Tubular	Qtz-Fd-calc-H-K-Sm
Buitrera8	70.85	16.32	1.16	0.005	0.44	0.31	1.73	1.73	0.054	<0.01	7.40		Tubular	Qtz-Fd-H-K

	LOI	SiO_2	Al_2O_3	TiO_2	Fe_2O_3	K_2O	CaO	V_2O_5	ZrO_2	SO_3	ZnO	CuO	Ga_2O_3	SrO
Comp Sample	11.77	48.08	37.30	1.37	0.59	0.18	0.16	0.05	0.03	0.03	0.009	0.008	0.007	0.002

the same pattern as the fresh rocks. Due to this characteristic, two types of altered rocks may be recognized in the Mamil Choique and Buitrera areas (Cravero et al., 2012).

The trace element content and the ratios Zr vs. Ti, Cr + Nb vs. $TiO_2 + Fe_2O_3$, and Ce + Y + La vs. Ba + Sr (Fig. 5) of halloysite samples from Buitrera and Mamil Choique areas do not differ significantly. This suggests that both deposits might have been formed by the same genetic process. Although some variations were found between Buitrera and Mamil Choique areas, those are due to differences in the degree of alteration.

Ti may be released from a primary mineral in the parent rock (biotite, for example) during either hypogenic or supergenic kaolinization. However, as supergenic alteration seems to be more efficient, the Ti content in kaolinite has been used to discriminate between the two processes (Dill et al., 1997). Because Zr behaves like a geochemically immobile element in superficial conditions, it is also a good indicator of the degree of weathering of the parent rock. Consequently, kaolin samples with high Ti and Zr contents point to a superficial environment of formation (Fig. 5c).

Compared to hypogenic deposits, kaolin deposits of supergenic origin usually present higher concentration of Nb and Cr (Cr + Nb > 100 ppm). This is due to the concentration of Nb in Ti-bearing minerals and to the substitution of Ti in TiO_2 and of Fe in goethite by Cr during supergenic kaolinization. On the other hand, as Ti and Fe tend to concentrate preferentially in supergenic kaolin, the amount of Ti + Fe present in this type of deposit is usually higher than 1% by weight (Dill et al., 1997). The Cr + Ni vs. Ti + Fe ratios presented in Fig. 5a show that the analyzed samples plot between the values discussed above, that is, they plot within the theoretical field for kaolinites of supergenic origin.

The low Sr and Ba concentrations (Sr + Ba between 13 and 975 ppm) are related to deposits of supergenic origin (Dill et al., 1997). Ce + La + Y contents in the analyzed samples are variable, reaching up to 500 ppm in the Meliqueo mine (Fig. 5b). Then, considering the trace-element geochemistry, the wide range and the high contents of Ce + Y + La and Nb + Cr, the latter especially in the Buitrera mine, are interpreted as the result of supergenic origin in all the deposits studied.

The stable isotope composition of kaolinites may also help to understand their origin, provided that the mineral retains the isotopic composition attained during the formation process (Savin and Lee, 1988; Shepard and Gilg, 1996).

The O and H stable isotope composition of three samples, two halloysites and one kaolinite, is shown in Fig. 6. $\delta^{18}O$ and δD values range from +18.3 to +19.8 ‰ and from −70 to −93.5 ‰, respectively. Both $\delta^{18}O$ and δD values are similar to those reported by Cravero et al. (1991) in kaolinites from deposits of residual origin in the Santa Cruz and Chubut provinces ($\delta^{18}O$ from +16.5 to +18.8 ‰ and δD from −57.5 to −86.5 ‰). These results are clearly different to those reported by Marfil et al. (2005, 2010) and Grecco et al. (2012, 2014) for kaolins of hydrothermal origin.

According to Savin and Lee (1988), the isotopic composition of kaolinite may reflect the geologic conditions during its formation, provided the mineral did not undergo isotopic changes after its deposition. Thus, the oxygen isotope composition in kaolinites of sedimentary origin usually varies from +19 to +23 ‰, and kaolinite from residual deposits has a $\delta^{18}O$ between +15 and +19 ‰ (Murray and Janssen, 1984); these values are compatible with a meteoric origin at temperatures between 20 and 25 °C. Therefore, the $\delta^{18}O$ values of the analyzed samples allow us to confirm that halloysite deposits were formed under superficial

Please cite this article as: Cravero, F., et al., Spheroidal halloysites from Patagonia, Argentina: Some aspects of their formation and applications, Appl. Clay Sci. (2015), http://dx.doi.org/10.1016/j.clay.2016.01.011

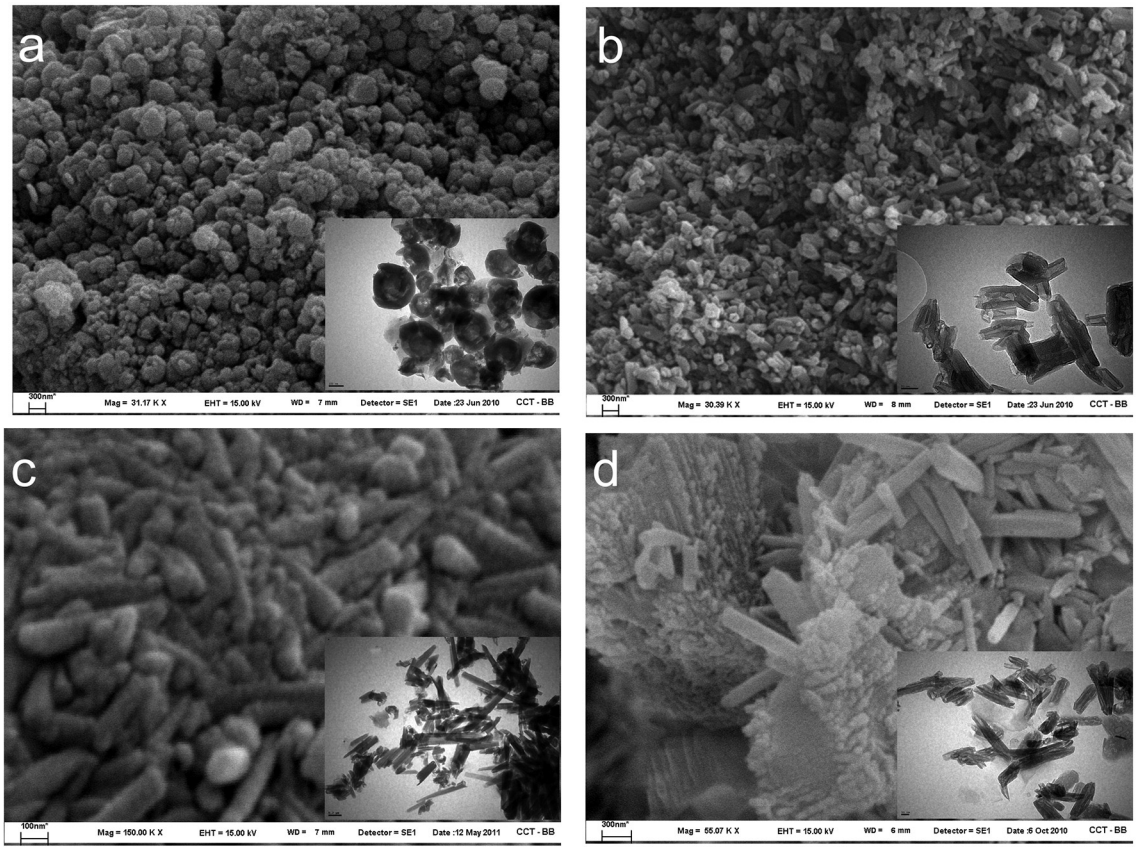

Fig. 4. SEM photomicrography. a. spheroidal halloysite of Mamil Choique area. b, c, d. tubular halloysite in Meliqueo, Alfa and Buitrera respectively. Figures a and b are taken from Cravero et al. (2012).

conditions in a warm climate. Global warm and humid climatic conditions (see Le Roux, 2012a, 2012b for a review) have been suggested for the early Paleogene, indicating that the alteration should have proceeded no longer after the volcanic event that produced the pyroclastic rocks of Huitrera Formation (Eocene age), when most of the deposits were formed.

3.2. Industrial applications

The only active mine at present is Pama. The mined mineral is used to manufacture a product known as Duoprotect, which acts as a sunscreen when sprayed on fruit. It was also used in the ceramic industry to enhance slurry viscosity (only 6% was added).

The mined (Comp Sample) mineral has been tested for different purposes. It is composed of halloysite, and minor quartz, cristobalite and smectite (determined as ferruginous beidellite by Cravero et al. (2014a)).

Because of its nanometer size, halloysite has been modified by means of different organic compounds to obtain a nanocomposite to be used in different industries. Zacur et al. (2011) used a sample with almost 100% tubes and mixed it with PLA (polylactic acid). They found that halloysite produces the nucleation of PLA crystals.

Fernández (2012), Fernández et al. (2012) demonstrated the success in using modified clays in the synthesis of controlled release fertilizers (CRF) by controlling water solubility of the fertilizer. Distinctive coating and occlusion technologies, in which urea was coated with nanocomposite materials, were applied. In the synthesis of the nanocomposite, a modified Comp Sample and a bentonite were the inorganic fraction that granted varying degrees of hydrophobicity. All the formulated coatings allowed a more slowly discharge than that of the natural fertilizer urea.

Retention of emulsified oil in water was investigated using a modified Comp" Sample (hydrophobic) with three different technologies: contact batch (Fernández et al., 2009a), dynamic membranes and packed columns (Ontivero et al., 2010). High percentages of emulsified hydrocarbon removal (above 96%) were obtained in all cases. Fernández et al. (2015) published the procedure to modify the Comp Sample by immobilization of ligands containing vinyl (C═C) groups by covalent grafting with surface silanol groups. The results indicated that the vinyl groups grafted at the mineral edges changed the hydrophilic nature of the clay mineral into hydrophobic. The vinyl group was chosen due to its great affinity for hydrocarbons.

Fernández and Gamboa (2015) chemically modified the Comp Sample by silanization to impart distinctive interface electrical properties, and tested it as adsorbent of the A6 Petrostep surfactant used in enhanced oil recovery techniques by injection of chemicals. The selected silane permitted the covalent binding of a diamino group to the surface of the material, making the resulting material amphoteric. Sedimentation and adsorption tests indicated the potential of the modified material to carry out the sought removal.

Adsorption with activated carbon is one of the techniques most widely used worldwide for the treatment of water, with the disadvantage of its high cost. Waters from industries such as mining, metal coatings and others are contaminated with various metals. In order of importance in terms of abundance, they are salts of lead, zinc, mercury, silver, nickel, cadmium and arsenic, being very toxic to terrestrial and aquatic flora and fauna.

A new study focused on the use of halloysite in the extraction of heavy metals. Yavuz et al. (2003) studied the removal of copper (Cu^{++}), nickel (Ni^{+}), cobalt (Co^{++}) and manganese (Mn^{++}) from aqueous solutions using a natural kaolinite as adsorbent. The results indicated that kaolinite has affinity to adsorb these metals in the following order: $Cu^{++} > Ni^{++} > Co^{++} > Mn^{++}$. Adebowale et al. (2005) showed

Please cite this article as: Cravero, F., et al., Spheroidal halloysites from Patagonia, Argentina: Some aspects of their formation and applications, Appl. Clay Sci. (2015), http://dx.doi.org/10.1016/j.clay.2016.01.011

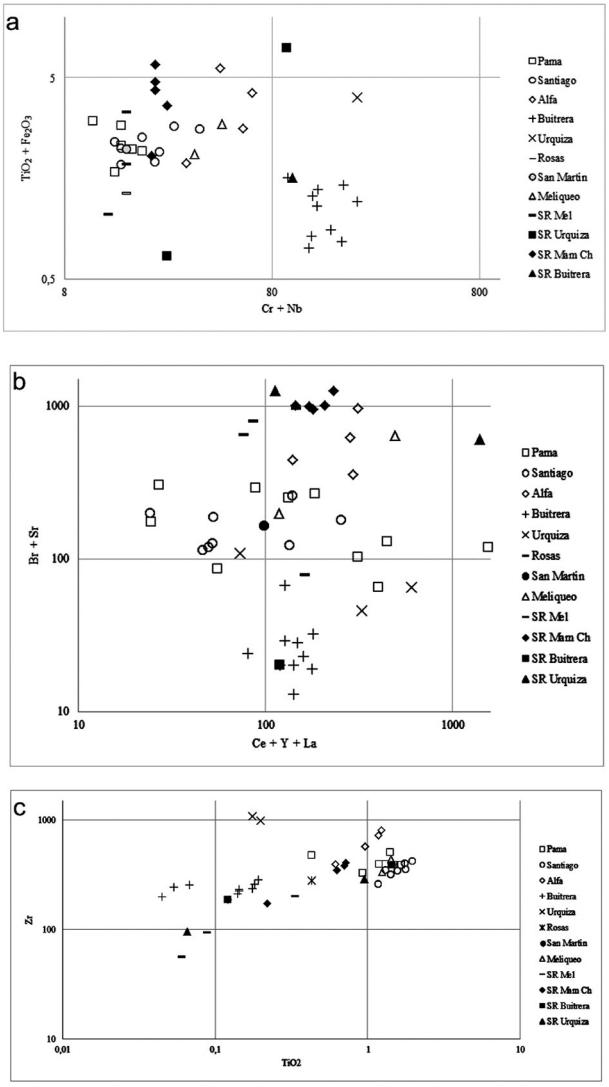

Fig. 5. Data plot from the studied mines (Dill et al., 1997). a. ($TiO_2 + Fe_2O_3$) vs. (Cr. + Nb). b. (Ba + Sr) vs. (Ce + Y + La). c. Zr vs. TiO_2.

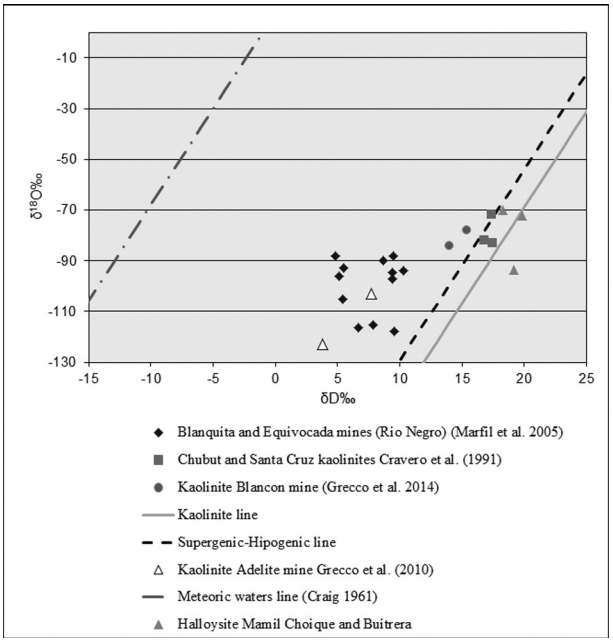

Fig. 6. δ ^{18}O and δD values in halloysite/kaolinite from Buitrera and Mamil Choique are compared with those of kaolin deposits from Patagonia studied in previous works.

that the modification of kaolin with sulfate and phosphate anions improves the adsorption of lead (Pb^{++}), cadmium (Cd^{++}), zinc (Zn^{++}) and copper (Cu^{++}). Suraj et al. (1998) reported that kaolinite modified by heat treatment and subsequent acid activation (thermoacid treatment) can be used for the retention of cadmium (Cd^{++}) and copper (Cu^{++}). Cu^{++} retention increased significantly in the activated kaolinite sample.

Although there are several methods of modification, silanization, a well-known strategy for oxides (Yoshida et al., 2001; Fernández et al., 2009b) is being increasingly applied to clay minerals (Sayılkan et al., 2004; He et al., 2005; Shen et al., 2007; Ferreira Guimaraes et al., 2009). The success of silanization depends on the structure of the selected mineral, the functionality of the silane component, and the route to synthesis of the reaction.

3.2.1. Halloysite modification

In this work, the Comp Sample was modified by silanization without any pretreatment covalently linking the component 3-aminopropyltrimethoxysilane (APS). Since the amino group of the APS forms complexes with heavy metals (Fernández et al., 2010; Parolo et al., 2013), halloysite was tested for the removal of Ag^{+} ions from aqueous solution. For this experiment, a 500 mL capacity reactor was heated by an oil bath and agitated by an electronic magnetic stirrer with heat(Velp Scientifica). A proper amount of clay was loaded into the reactor, the temperature was slowly raised to the desired value, and then the silanization agent was added. The silanization reaction with APS was carried out using ethanol/water as solvent solution. Reaction time was 6 h. The reaction temperature was kept constant below the boiling point of the solvent with a Velp controller. The cooling water temperature in the condenser was controlled by a Polystat circulating bath (Cole-Parmer), maintaining a constant temperature of 80 °C during the reaction, in order to reflux the evaporated solvent, but allowing the elimination of methanol (by-product of the reaction). Clay was washed three times with fresh solvent. During each of these stages the solid was stirred for 5 h, allowing it to settle, and then the supernatant fluid was separated. The drying operation was conducted in a rotoevaporator. There was an important change in the electrical properties caused by the surface anchoring of APS (Fig. 7). The Comp" Sample presented negative potential in all the pH range studied, while the Comp Sample-APS exhibits an amphoteric behavior. At low pH, the amino group was protonated, resulting in a positive potential. At higher pH the modified sample took a negative potential lower than that of the natural sample. This behavior seems to indicate that the surface coating with APS was not complete. At high pH values, the modified sample behaved like the natural one but with fewer exposed hydroxyl groups,

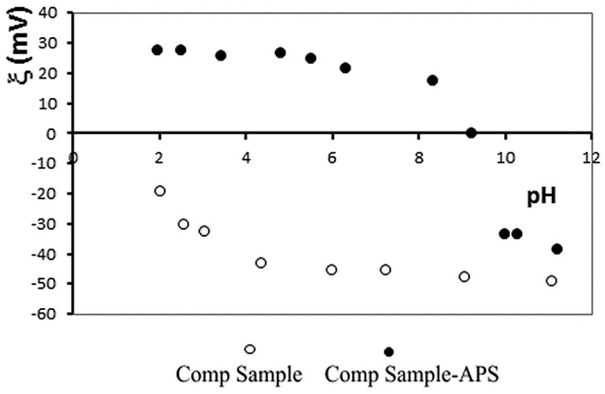

Fig. 7. Electrical properties of Comp Sample and CompSample-APS".

Please cite this article as: Cravero, F., et al., Spheroidal halloysites from Patagonia, Argentina: Some aspects of their formation and applications, Appl. Clay Sci. (2015), http://dx.doi.org/10.1016/j.clay.2016.01.011

since a certain fraction of them was shielded by silane. The Comp Sample-APS presented an isoelectric point at pH ≈ 9.2. (See Fig. 7.)

3.2.1.1. Structural Characterization. By grafting silane onto halloysite, the nonexpansion of the mineral layers was demonstrated by X-ray diffraction. The XRD patterns of halloysite before and after grafting are shown in Fig. 8. The basal spacing was 7.2 Å for the APS sample. The diffraction patterns show that the interlayer distances of APS-modified clay sample remained unchanged, indicating that intercalation of APS into the interlayer of halloysite did not occur. This result indicates that most of the interlayer inner-surface AlOH groups of halloysite were unavailable for grafting, since they were blocked by the strong hydrogen bonds between layers, in agreement with Yuan et al. (2008).

3.2.1.2. FTIR Analysis. When analyzed by IR (Fig. 9), the Comp Sample presented the characteristic peaks (Madejová and Komadel, 2001). Compared to the unmodified Comp Sample, the APS-modified Comp Sample (Comp Sample-APS) exhibited some new FTIR peaks, such as the CH_2 stretching around 2939 cm^{-1} (3020–2939 cm^{-1}), the OCH_3 stretching (unhydrolyzed methoxy group) at 2850 cm^{-1}, the deformation CH_2 vibration at 1494 cm^{-1}, the deformation SiCH vibration at 1330 cm^{-1}, the stretching of NH_2 at 3300 cm^{-1}, and the deformation NH_2 vibration at 1525 cm^{-1}. All of these observations show the presence of APS moieties in the modified clay.

As is known, in water silane is easy to hydrolyze and condense among silane molecules. After hydrolysis, the configuration of silane will be changed with polymerization. Because of the presence of the FTIR peak corresponding to unhydrolyzed methoxy group, the APS molecules could not hydrolyze thoroughly.

Compared to the spectrum of the "comp" sample, the modified sample showed a decrease in the intensity of the OH stretching band (3696 and 3656 cm^{-1}) of the inner-surface AlOH groups. This indicates that the modification was accompanied by the consumption of inner-surface AlOH, that is, grafting took place between these groups and the hydrolyzed APS.

The XRD characterization showed that the inner-surface AlOH groups in the interlayer region were not available for grafting, suggesting that the vast majority of grafting occurred on the AlOH groups at the internal wall, or on the AlOH or SiOH groups at the edges or external surface defects, which are accessible by APS. This proposal is supported

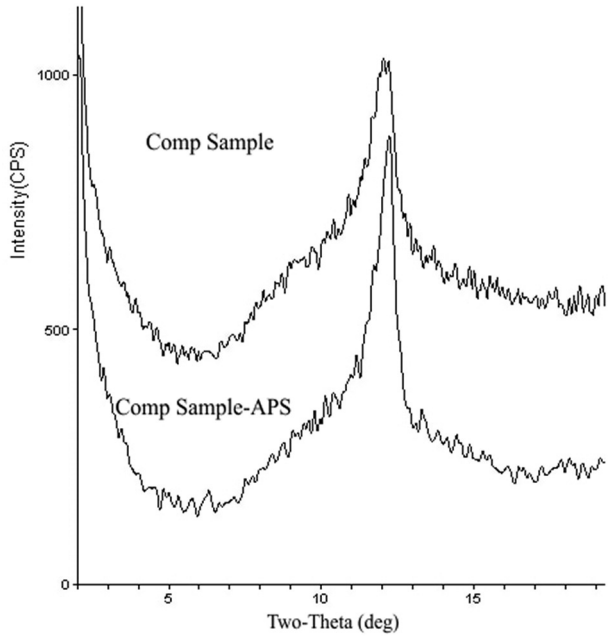

Fig. 8. XRD of the raw (Comp Sample) and modified halloysite (Comp Sample-APS).

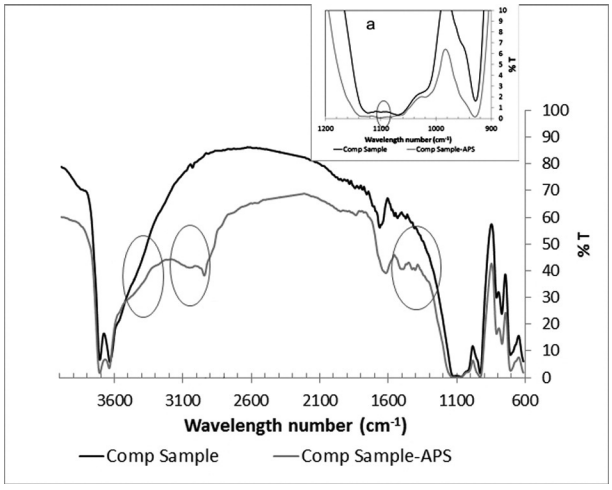

Fig. 9. Infrared (IR) of raw and modified halloysite Comp Sample and Comp Sample-APS".

by the decrease in intensity of the Si-O-Si peak at 1088 and 1025 cm^{-1} (Fig. 9). In addition, hydrolyzed APS might also have oligomerized or even polymerized with surface water and the oligomerized APS further reacted with grafted APS to form a cross-linked network. The network was formed mainly through covalent bonds, but hydrogen bonding might have been another way for oligomerized APS to combine with halloysite or grafted APS. This is supported by the existence of NH_2 vibration bands at 3360 and 3300 cm^{-1}, which have been discussed and proposed as an indication of the formation of hydrogen bonding (Yuan et al., 2008).

3.2.1.3. Thermal analysis of grafted halloysite. To gain more insight into the grafting process, thermal analyses were used to determine the amount of silane molecules chemically anchored on the clay edges

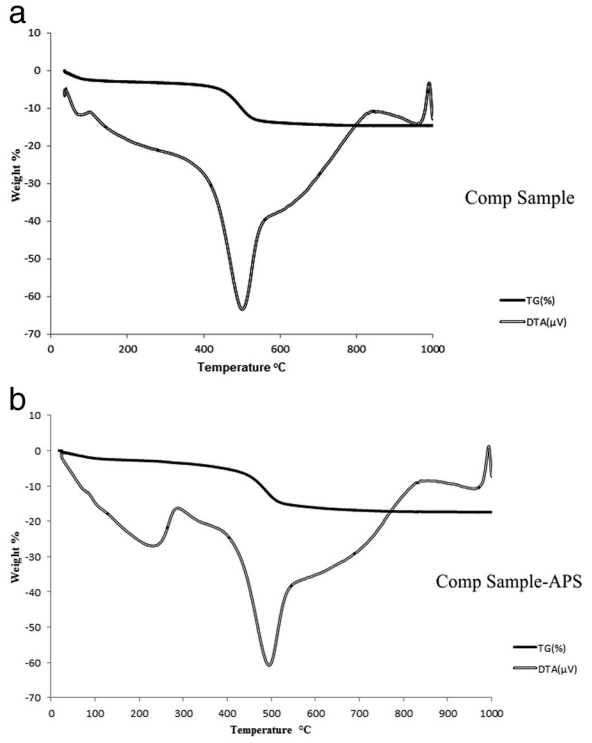

Fig. 10. a. DTA-TG of raw halloysite (Comp Sample) b. DTA-TG of modified halloysite (Comp Sample-APS).

Please cite this article as: Cravero, F., et al., Spheroidal halloysites from Patagonia, Argentina: Some aspects of their formation and applications, Appl. Clay Sci. (2015), http://dx.doi.org/10.1016/j.clay.2016.01.011

after extensive washing of the unreacted coupling agent. In addition, the modified sample was dried at 130 °C in a vacuum oven for 24 h before the thermal analyses.

Thermogravimetric analysis (TG) was provided as a simple method to measure the content of silane and physisorbed water, (Shen et al., 2007). This method is based on the assumption that the dehydration and dehydroxylation reactions correspond to the two discrete mass loss steps in TG curves and they do not overlap each other. Silylation yields were determined by TG. Each sample was heated at 10 °C/min up to 1000 °C to eliminate all the organosilanes bonded on the surface, Zubakova et al. (1987). All runs were performed in an O_2 atmosphere.

The TG of the Comp Sample is shown in Fig. 10a. The DTA curve of the "comp" sample displays two peaks at ca. 81.2 and 500.9 °C, assigned to the loss of physically adsorbed water (2.34%) and the dehydroxylation of halloysite (11.52%). For the Comp Sample there was a small mass loss (ca. 0.6%) in the range 200–410 °C attributed to the loss of organic matter as the natural clay was used as received without any purification or cleaning pretreatment.

The major mass loss (Loss-D: 10.9%)was resolved in the temperature range 410–700 °C and was assigned to the dehydroxylation of structural AlOH groups of halloysite. Therefore, a greater mass loss than expected should be attributed to evaporation and/or decomposition of silane.

For the modified sample, Comp Sample-APS (Fig. 10b) three mass losses were resolved, corresponding to DTA peaks al 231, 287, 410 and 495 °C. Because the modified clays were dried in a vacuum oven, it is noted that the peak corresponding to the loss of physically adsorbed water disappeared after grafting with APS.

The first mass loss (Loss-1) in the range 50–231 °C is attributed to hydrogen-bonded APS existing in the cross-linking framework. The hydrogen-bonded APS was much less thermally stable than the covalently bonded APS, and decomposed at a lower temperature. The mass loss (Loss-2) occurring from 230 to 410 °C, corresponding to the well resolved DTA peak at 287 °C and the broad DTA peak between 320 and 410 °C, implies that thermal decomposition occurred in several stages. These stages include decomposition of the APS species grafted onto SiOH and AlOH groups on edges or the external surface, the oligomerized APS, and the APS grafted on AlOH groups at the internal surface of halloysite.

The decomposition of different APS species appears to be a slow and gradual process and partially overlapped, leading to a complex multistep mass loss, and thus an accurate definition of the boundary between different processes could not be achieved, in agreement with Yuan et al. (2008).

However, the value of Loss-M (Loss –M = Loss-1 + Loss-2), Table 2, in the range 50–410 °C of the modified sample is a simple indication of the quantity of introduced organics.

The third mass loss (Loss-D) over the range 410–700 °C corresponds to dehydroxylation of the residual structural AlOH groups, including the inaccessible inner AlOH groups, the inner-surface AlOH in the interlayer region, and also the unreacted AlOH groups on the inner surface of the lumen for halloysite nanotubes, (Yuan et al., 2008). This is the main observation arising from this part of the TG curves. It is noted (Table 2) that the mass loss for the modified sample was greater than the equivalent mass loss for the unmodified sample. This indicates that Loss-D must have included some organic decomposition reactions that extended beyond 410 °C, in agreement with Yuan et al. (2008).

Table 2
Mass losses of raw and modified halloysite (Comp sample and Comp sample-APS).

	Comp sample	Comp sample-APS
Loss-1 (%)	–	2.15
Loss-2 (%)	–	2.14
Loss-M(%)	0.6	4.30
Loss-D(%)	10.9	11.55
Content of loaded APS (%)		4.95

The mass quantity of grafted APS, evaluated as the difference between the weight loss for silylated clays and for unmodified ones at 700 °C without considering the amount of water adsorbed, was 4.95%. This result is in good agreement with the content of APTES loaded onto natural halloysite nanotubes (4.97%) reported by Yuan et al. (2008). In this work, the raw clay sample was purified by repeated sedimentation processes to remove quartz impurities, followed by drying at 110 °C for 12 h, grinding and rehydratation under ambient condition for 48 h.

3.2.2. Adsorption capacity of the natural and modified halloysite

The adsorption capacity and kinetics of silver ions were investigated for both natural (Comp Sample) and modified (Comp Sample-APS) halloysites, by contacting solutions with an initial concentration of 50 ppm of Ag^+ (Co) at free pH batch, maintaining a dosage of 1.7 (g solid/L solution). The concentration of Ag^+ was monitored by measuring the supernatant using the Volhard Protocol (Domínguez et al., 2002), which determined the amount adsorbed by mass balance. The results (Table 3), where the uptake (qt) is defined as the amount of Ag^+ retained in the solid per gram of solid, as a function of time (qt = Ag^+ retained per mg/g of solid), show that the modified sample tripled the adsorption capacity of Ag^+, reaching a maximum uptake at the equilibrium point 15.20 mg/g (qe) against 4.71 mg/g for the natural specimen. Fernández et al. (2010) modified a bentonite with APS by the same chemical route. By keeping the parameters of dosage of modified clay and concentration of Ag + in the contact solution, the adsorption capacity was 10 pm mg/g (qe). This increase against the modified halloysite is explained by an increase in the performance of silanization (7.4%).

For the silanized sample, the increase in retention can be explained considering that the ion exchange mechanism was enforced by the formation of a complex between the silver ion and the amino group of silane, with no electrostatic attraction because of the positive Zeta potential in the pH tested (Fig. 7).

3.2.3. Ceramic properties

In the ceramic industry, the presence of ferruginous beidellite in the clay is not desired because it produces a higher contraction (Table 4).

Table 3
Variation in the concentration of Ag^+ as a function of time, ads: adsorption, (qt) = amount of Ag + retained in the solid per gram of solid, as a function of time, (qt = Ag + retained mg/g of a solid) (qe) = equilibrium point.

Sample	pH	Time t(min)	Concentration C(t) Ag^+ (mg/L)	Uptake qt (mg/g)	% ads
Comp	$pH_i = 6$	0	50	0.00	0.00
		60	48	1.18	4.00
		120	47	1.76	6.00
		160	46	2.35	8.00
		240	44	3.53	12.00
		380	44	3.82	13.00
		1000	43	4.00	13.60
		1440	43	4.12	14.00
		2000	43	4.29	14.60
		2880	43	4.29	14.60
		3500	42	4.71	16.00
	$pH_f = 6$	4320	42	4.71	16.00
Comp + APS	$pH_i = 6.3$	0	50	0.00	0.00
		60	35	9.00	30.60
		120	27	13.71	46.60
		160	27	13.82	47.00
		240	26	14.12	48.00
		380	26	14.24	48.40
		1000	26	14.35	48.80
		1440	25	14.71	50.00
		2000	25	15.00	51.00
		2880	24	15.29	52.00
		3500	24	15.29	52.00
	$pH_f = 6.7$	4320	24	15.29	52.00

Please cite this article as: Cravero, F., et al., Spheroidal halloysites from Patagonia, Argentina: Some aspects of their formation and applications, Appl. Clay Sci. (2015), http://dx.doi.org/10.1016/j.clay.2016.01.011

Table 4
Modal diameter, CEC, brightness, contraction, resistance, pyrometric cone equivalent (PCE) and linear thermal dilatation tested on "comp" sample.

Modal diameter (μm)	0.99			
CEC	13.4 meq/100 g			
Brightness	72%			
Contraction (1230 °C)	14%			
Resistance (kg/cm^2)				
Green	3			
Dry	11			
Fired	35			
Pyrometric cone equivalent (PCE)	33 (1741 °C)			
Linear thermal dilatation	**On heating**			
	Temp./°C	**(dL/Lo) %**	**Interval T(°C)**	**α (°C^{-1} 10^{-8})**
	30	0.00	30–100	2.05
	100	0.02	100–200	−0.23
	200	0.02	200–300	6.06
	300	0.08	300–400	2.60
	400	0.10	400–500	−12.18
	500	−0.02	500–600	−125.6
	600	−1.27	600–700	−50.02
	700	−1.78	700–800	−39.53
	800	−2.17	800–900	−51.79
	900	−2.69	900–1000	−373.86
	1000	−6.43		−62.00
	1100	−7.05	1100–1200	−313.21
	1200	−10.18	1200–1300	9.80
	1300	−10.08		
	1400	−9.99		
	1500	−9.88		

This contaminant is randomly distributed in the deposit, forming irregular "patches" from few cm to 1 m. The only possibility to remove it is by hand selection. Titanium oxide is another undesired component that is probably the main cause of the not very high whiteness (about 80%). In the samples (Table 1) from different parts of the deposit, TiO_2 varies between 0.93 and 1.97. Cravero et al. (2014b) analyzed the provenance of this titanium and concluded that it is present as fine to very fine grained anatase, and that some TiO_2 occurs in between kaolinite layers, but it is not found in halloysite spheroids. This feature opens the way to test a mechanical method to extract the undesired titanium, thus enhancing the brightness.

Therefore, to obtain a good ceramic product, hand selection, to guarantee the purest material, followed by a mechanical treatment to get rid of titanium should be used.

4. Conclusions

- In the study area, western Patagonia, the processes that have altered rocks from Permian to Eocene occurred during the early Paleogene in a warm, humid climate.
- Halloysite predominates in volcanic-pyroclastic parent rocks, whereas kaolinite is found as an alteration product in plutonic rocks.
- The modification of the studied spheroidal halloysite seems to be similar to that performed on tubular halloysites reported elsewhere.
- Chemical modification of the mined mineral has given good results for petroleum and Ag removal from contaminated waters.
- The use of this mineral in the ceramic industry is constrained by the presence of iron smectite and titanium oxides. Only hand selection and mechanical treatment can guarantee a good product.

Acknowledgments

We thank CETMIC, CONICET and Comisión de Investigaciones Científicas from the province of Buenos Aires and the Geology Department of the Universidad Nacional del Sur. We are and will be greatly indebted to Dr. Haydn H. Murray for all he did for the clay science. In particular, he helped the senior author a lot during her career and encouraged her to study kaolins and their applications. The authors thank the reviewers (especially the detailed revision by reviewer 2) for their comments, which helped improve this work.

References

Adamo, P., Violante, P., Wilson, M.J., 2001. Tubular and spheroidal halloysite in pyroclastic deposits in the area of the Roccamonfina volcano — Southern Italy. Geoderma 99, 295–316.
Adebowale, K.O., Unuabonah, I.E., Olu-Owolabi, B.I., 2005. Adsorption of some heavy metal ions on sulfate- and phosphate-modified kaolin. Appl. Clay Sci. 29, 145–148.
Askenasy, P.E., Dixon, J.B., McKee, T.R., 1973. Spheroidal halloysite in Guatemalan soil. Soil Sci. Soc. Am. Proc. 37, 799–803.
Bailey, S.W., 1989. Halloysite—a critical assessment. In: Farmer, V.C., Tardy, Y. (Eds.), Proceedings of the International Clay Conference; Strasbourg, France. Sci. Geol. Mem. 86, pp. 89–98.
Churchman, G.J., Carr, R.M., 1975. The definition and nomenclature of halloysites. Clay Clay Miner. 23, 382–388.
Churchman, G.J., Lowe, D.J., 2012. Alteration, formation, and occurrence of minerals in soils. In: Huang, P.M., Y., L., Sumner, M.E. (Eds.), Handbook of Soil Sciences, second ed. Vol. 1, Properties and Processes 20. CRC Press (Taylor & Francis), Boca Raton, FL, pp. 1–20.72.
Churchman, G.J., Theng, B.K.G., 1984. Interactions of halloysites with amides: mineralogical factors affecting complex formation. Clay Miner. 19, 161–175.
Churchman, G.J., Whiton, J.S., Claridge, G.G.C., Theng, R.K.G., 1984. Intercalation method using formamide for differentiation halloysite from kaolinite. Clay Clay Miner. 32, 241–248.
Churchman, G.J., Pontifex, I.R., McClure, S.G., 2010. Factors influencing the formation and characteristics of halloysites or kaolinites in granitic and tuffaceous saprolites in Hong Kong. Clay Clay Miner. 58, 220–237.
Condie, K.C., Dengate, J., Cullers, R.J., 1995. Behavior of rare earth elements in a paleoweathering profile on granodiorite in the front range, USA. Geochim. Cosmochim. Acta 59, 279–294.
Cravero, M.F., Domínguez, E., Murray, H.H., 1991. Valores δO18 y δD en caolinitas, indicadores de un clima templado moderado Durante el Jurásico Superior-Cretácico Inferior de la Patagonia, Argentina. Rev. Asoc. Geol. Argent. 46, 20–25.
Cravero, F., Martínez, G.A., Pestalardo, F., 2009. Yacimientos de halloysita en Mamil Choique, Provincia de Río Negro, Patagonia. Rev. Asoc. Geol. Argent. 65, 586–592.
Cravero, F., Maiza, P., Marfil, S., 2012. Halloysite in Argentinian deposits. Origin and textural constraints. Clay Miner. 47, 329–340.
Cravero, F., Marfil, S., Ramos, C., Maiza, P., 2014a. Coexistence of halloysite and iron-bearing clays in an altered ignimbrite, Patagonia, Argentina. Clay Miner. 49, 377–389.
Cravero, F., Marfil, S., Maiza, P., 2014b. Distribución del titanio en los yacimientos de halloysita del área de mamil choque prov. de Río Negro, Argentina, II simposio de arcillas. Las arcillas y el hombre: geología, combustibles fósiles y cultura material. XIX Congreso Geológico Argentino, Junio 2014, Córdoba. Actas, p. S1-1.
Dill, H.G., Bosse, H.R., Henning, H., Fricke, A., 1997. Mineralogical and chemical variations in hypogene and supergene kaolin deposits in a mobile fold belt the central Andes of northwestern Peru. Mineral. Deposita 32, 149–163.
Domínguez, L., Yue, Z., Economy, J., Mangun, C.L., 2002. Design of polivinyl alcohol mercaptyl fibers for arsenite chelation. React. Funct. Polym. 53, 205–215.
Fernández, L., 2012. INNOVAR, concurso Nacional de innovaciones, ID 12410. Producto Para Descarga Lenta de Urea Basado en una Arcilla Químicamente Modificada.
Fernández, L., Gamboa, N., 2015. Síntesis de un adsorbente de sufractantes aniónicos en escenarios de recuperación mejorada de petróleo. Congreso Latinoamericano Ingeniería y Ciencias Aplicadas. San Rafael, Mendoza, Argentina. April 15–17.
Fernández, L., Sánchez, M., De la Cruz, C., Ontivero, M., Santoni, D., Berti, P., Rozas, C., Cravero, F., 2009a. Síntesis, caracterización y aplicación de nanotubos hidrofóbicos. CLICAP-Congreso Latinoamericano de Ingeniería y Ciencias Aplicadas- Mendoza, Argentina. March, 18–20, 2009 Code: 24Q.
Fernández, L., Soria, C., Sánchez, M., Pérez, G., Palacio, L., Prádanos, P., Hernández, A., Lozano, A.E., 2009b. Funcionalization of γ-alumina cores by polyvinylpirrolidone. Properties of the resulting biocompatible nanoparticles in aqueous suspension. J. Nanoparticle Res. 11 (2), 341.
Fernández, L., Sánchez, M., De la Cruz Vivanco, C., Zajonskovsky, I., Parolo, M., Baschini, M., Cravero, F., 2010. Funcionalización de una esmectita con un grupo amino. Aplicaciones en la Protección de la Salud y el Medioamgiente. VI Congreso Argentino de Ingeniería Química-CAIQ2010, Mar del Plata, Argentina. September 26–29.
Fernández, L., Moll, G., Sánchez, M., 2012. Descarga lenta de urea a partir de formulaciones con nanocompuestos polímeros-arcillas modificadas. Congreso Internacional de Ciencia y Tecnología Ambiental y I Congreso Nacional de la Sociedad Argentina de Ciencia y Tecnología Ambiental, May 28-June 1, Mar del Plata-Argentina.
Fernández, L.G., Cravero, F., Sánchez, M., De la Cruz, C., Gatti, M., 2013. Síntesis y caracterización de una halloysita modificada con viniltrimetoxisilano. 13er Congreso Internacional en Ciencia y Tecnología de Metalurgia y Materiales, Puerto Iguazú, Argentina.
Fernández, L., Cravero, F., Sánchez, M.P., De la Cruz Vivanco, C., Gattia, M., 2015. Synthesis and Characterization of Vinyltrimethoxysilane-Grafted Non-Swelling Clay. Procedia Materials Science 8, 414–423.

Please cite this article as: Cravero, F., et al., Spheroidal halloysites from Patagonia, Argentina: Some aspects of their formation and applications, Appl. Clay Sci. (2015), http://dx.doi.org/10.1016/j.clay.2016.01.011

Ferreira Guimaraes, A., Ciminelli, V., Vasconcelos, W., 2009. Smectite organofunctionalized with thiol groups for adsorption of heavy metal ions. Appl. Clay Sci. 42, 410–414.
Galán, E., Fernández-Caliani, J.C., Miras, A., Aparicio, P., Márquez, M.G., 2007. Residence and fractionation of rare earth elements during kaolinization of alkaline peraluminous granites in NW Spain. Clay Miner. 42, 341–352.
Grecco, L., Marfil, S., Maiza, P., 2012. Mineralogy and geochemistry of hydrothermal kaolins from the Adelita mine, Patagonia (Argentina). Clay Miner. 47, 131–146.
Grecco, L., Marfil, S., Maiza, P., 2014. Geoquímica y mineralogía de un depósito de caolín del área de Los menucos, provincia de Río Negro. Rev. Asoc. Geol. Argent. 71, 201–209.
He, H., Duchet, J., Galy, J., Gerard, J.-F., 2005. Grafting of swelling clay materials with 3-aminopropyltriethoxysilane. J. Colloid Interface Sci. 288, 171–176.
Keeling, J.L., 2015. The mineralogy, geology and occurrence of halloysite. In: Pasbakhsh, P., Churchman, G.J. (Eds.), Natural Mineral Nanotubes, Properties and Applications. Apple Academic Press, Inc., Oakville, Canada, pp. 95–116.
Le Roux, J.P., 2012a. A review of tertiary climate changes in southern South America and the Antarctic peNinsula. Part 1: oceanic conditions. Sediment. Geol. 247-248, 1–20.
Le Roux, J.P., 2012b. A review of tertiary climate changes in southern South America and the Antarctic Peninsula. Part 2: continental conditions. Sediment. Geol. 247-248, 21–38.
Madejová, J., Komadel, P., 2001. Baseline studies of the clay minerals society source clays: infrared methods. Clay Clay Miner. 49, 410–432.
Marfil, S., Maiza, P., Cardellach, E., Corbella, M., 2005. Origin of kaolin deposits in the Los Menucos, Río Negro Province, Argentina. Clay Miner. 40, 283–293.
Marfil, S., Maiza, P., Montecchiari, N., 2010. Alteration zonation in Loma Blanca Kaolin deposit, Los Menucos, province of Rio Negro, Argentina. Clay Miner. 45, 157–169.
Murray, H., Janssen, J., 1984. Oxygen Isotopes — Indicators of Kaolin Genesis? Proceedings of the 27th International Geological Congress, 15, 287–303.
Nagasawa, K., 1978. Weathering of volcanic ash and other pyroclastic materials. In: Sudo, T., Shimoda, S. (Eds.), Clays and Clay Minerals of Japan. Elsevier, Amsterdam, pp. 105–145.
Nagasawa, K., Miyazaki, S., 1976. Mineralogical properties of halloysite as related to its genesis. In: Bailey, S.W. (Ed.), Proc. Int. Clay Conf. 1975, Mexico City. Applied Publishing, Wilmette, IL, pp. 257–265.
Nagasawa, K., Moro, H., 1987. Mineralogical porperties of halloysites of weathering origin. Chem. Geol. 60, 145–149.
Ontivero, M., Tobis, A., De la Cruz, C., Fernández, L., 2010. Síntesis de arcillas hidrofóbicas para la retención de hidrocarburos emulsionados en Agua. Congreso de Producción del Bicentenario. IAPG (Instituto Argentino del Petróleo y del Gas). May, 18–21, Salta, Argentina.
Papoulis, D., Tsolis-Katagas, P., Katagas, C., 2004. Progressive stages in the formation of kaolinite from halloysite in the weathering of plagioclase. Clay Clay Miner. 52, 271–285.
Parolo, M.E., Fernández, L.G., Zajonkovsky, I., Sánchez, M.P., Baschini, M., 2013. Antibacterial activity of material synthesized from clay minerals. Science Against Microbial Pathogens: Communicating Current Research and Technological Advances 1, pp. 144–151.
Quantin, P., Gautheyrou, J., Lorenzoni, P., 1988. Halloysite formation through *in situ* weathering of volcanic glass from trachytic pumices, Vico's Volcano, Italy. Clay Miner. 23, 423–437.
Rollinson, H., 1992. Using Geochemical Data: Evaluation, Presentation. University of Zimbabwe, Interpretation (352 pp.).
Savin, S.M., Lee, S., 1988. Isotopic studies of phyllosilicates. In: S.W., B. (Ed.), Hydrous Phyllosilicates (Exclusive of Micas)Reviews in Mineralogy 19. Mineralogical Society of America, Washington DC, pp. 189–223.
Sayılkan, H., Erdemoglub, S., Sener, S., Sayılkan, F., Akarsu, M., Erdemoglu, M., 2004. Surface modification of pyrophyllite with amino silane coupling agent for the removal of 4-nitrophenol from aqueous solutions. J. Colloid Interface Sci. 275 (2004), 530–538.
Shen, W., He, H., Zhu, J., Yuan, P., Frost, R.L., 2007. Grafting of montmorillonite with different functional silanes via two different reaction system. J. Colloid Interface Sci. 313, 268–273.
Shepard, S.M.F., Gilg, H.A., 1996. Stable isotope geochemistry of clay minerals. Clay Miner. 31, 1–24.
Singer, A., Zarei, M., Lange, F.M., Stahr, K., 2004. Halloysite characteristics and formation in the northern Golan heights. Geoderma 123, 279–295.
Soma, M., Churchman, G.J., Theng, B.K.G., 1992. X-ray photoelectron spectroscopic analysis of halloysites with different composition and particle morphology. Clay Miner. 27, 413–421.
Sudo, T., Yotsumoto, M., 1977. The formation of halloysite tubes from spheritic halloysite. Clay Clay Miner. 25 (155–159), 155–159.
Suraj, G., Iyer, C.S.P., Lalithambika, M., 1998. Adsorption of cadmium and copper by modified kaolinites. Appl. Clay Sci. 13, 293–303.
Tazaki, K., 1982. Analytical electron microscopic studies of halloysite formation processes-morphology and composition of halloysite. Proc. Int. Clay Conf. Bologna, Pavia, pp. 573–584.
Tazaki, K., Asada, R., 2003. Microbes associated with clay minerals-formation of bio-halloysite. In: Domínguez, E.A., Mas, G.R., Cravero, F. (Eds.), 2001. A Clay Odissey, Proceedings of the 12th International Clay Conference. Bahía Blanca, Argentina. Elsevier, Amsterdam, pp. 569–576.
Tomura, S., Shibasaki, Y., Mizuta, H., Kitamura, M., 1985. Growth conditions and genesis of spherical and platy kaolinite. Clay Clay Miner. 33, 200–206.
Yavuz, O., Altunkaynak, Y., Güzel, F., 2003. Removal of copper, nickel, cobalt and manganese from aqueous solution by kaolinite. Water Res. 37, 948–952.
Yoshida, W., Castro, R.P., Jeng-Dung, J., Cohen, Y., 2001. Multilayer alkoxysilane of oxide surfaces. Langmuir 17, 5882–5888.
Yuan, P., Southon, P.D., Liu, Z., Green, M.E.R., Hook, J.M., Antil, S.J., Kepert, C.J., 2008. Functionalization of halloysite clay nanotubes by grafting with aminopropyltriethoxysilane. J. Phys. Chem. C 112, 15742–15751.
Zacur, R., Leobono, M., Dailoff, M.C., Miranda, M.A., Ercoli, D.R.,., Cravero, F., Goizueta, G.S., 2011. Análisis Mediante WAXS de la modificación de halloysita. VII Reunión de la Asociación Argentina de Cristalografía - San Carlos de Bariloche, Noviembre 2011.
Zubakova, L.B., Borisova, V.N., Koroleva, S.K., Davydox, V.Y., Filatova, G.N., 1987. Study of the chemistry of the surface of an adsorbent based on silicon and N-vinylpyrrolidone. Zh. Prikl. Khim. 60, 1491–1494.

Please cite this article as: Cravero, F., et al., Spheroidal halloysites from Patagonia, Argentina: Some aspects of their formation and applications, Appl. Clay Sci. (2015), http://dx.doi.org/10.1016/j.clay.2016.01.011